B6 mice. Human *lcat* gene-transduced m-ccdPA was subcutaneously transplanted into B6 mice with fibrin glue. Immunostaining of LCAT showed that the m-ccdPA 14 days after transplantation survive and express human LCAT protein in B6 mice (Figure 3). The hLCAT expression was still detectable in the transplanted m-ccdPA 28 days after transplantation (data not shown). The IP-western analysis showed that hLCAT protein was detected at least up to 28 days after transplantation in the serum of mice. The mouse sera collected were analyzed for LCAT protein by IP-western blotting (Figure 4A). hLCAT protein was detected up to 28 days after transplantation. Densitometric analysis (Figure 4B) showed that from day4 to day7, the density became significantly decreased, and from Day7 the concentration of LCAT protein became relatively constant. The LCAT delivery into serum from m-ccdPA transplanted with fibrin glue was in comparable level with those with Matrigel. These results showed that fibrin glue, a clinically commonly available material, worked as a scaffold for *in vivo* delivery of hLCAT protein.

Discussion

For the development of a long-lasting protein replacement therapy by the gene-transduced ccdPA, clinically applicable scaffold is one of possible approach for the improvement of survival and/or secretion function of transplanted cells in the patients. Various types of materials have been proposed (Neuss et al., 2008; Malafaya et al., 2007; Mano et al., 2007) as scaffolds for cell transplantation. In this study, we have chosen fibrin glue among them because it is already commonly used in clinic with the fact that easy handling kit is commercially available. In order to evaluate the effect of fibrin glue as a scaffold in the survival and function of transplanted adipocytes, we established autologous model system using human *lcat* gene-transduced m-ccdPA. The results using the model mice showed that fibrin glue supported human enzyme delivery from the transplanted m-ccdPA in the equivalent level to Matrigel, which is known as an efficient scaffold in experimental models. Thus, fibrin glue could be one of candidates as a scaffold for clinical transplantation of h-ccdPA, which has been established for long time an enzyme replacement for the enzyme deficiency, particularly for LCAT deficiency to prevent the development of renal insufficiency and/or corneal opacity (Kuroda et al. submitted).

Preliminary experiments showed that hLCAT protein was secreted by its gene-transduced m-ccdPA *in vitro*, however, in contrast to h-ccdPA in mice, was hardly detectable in mouse serum probably because of the lower capability of secretion (see result). The integrated copy number and LCAT activity in the culture medium could be

elevated by approximately three folds with the condition suitable for m-ccd-PA in mice (see Figure 1). As a result, IP-western analysis was sensitive enough for the quantification of serum hLCAT protein in the mice, and indicated that the delivered protein is equivalent to those of 15 μg HDL (see Figure 2A). These optimizations enabled us to establish an *in vivo* mice model to monitor the effect of fibrin glue as a scaffold for the transplanted m-ccdPA. Adipogenic differentiation did not significantly affect the LCAT delivery and cell survival in this model using fibrin glue as a scaffold with m-ccdPA (see Figure 2B). In this context, our results may support that transplanted cells with fibrin glue were differentiated into adipocytes without adipogenic pretreatment (Cho et al. 2006, Torio-Padron et al. 2007). The immunohistochemical observation did not clearly shown that ccdPA would undergo adipogenic differentiation after transplantation, but transplanted ccdPA was certainly identified as LCAT-delivery cells in the transplanted site of the recipient mice (see Figure 3). The *lcat* gene transduced m-ccdPA/fibrin glue showed that the serum LCAT concentration decreased to one half in a week, and became relatively stable at 7-14 days after transplantation (see Figure 4). Thus, we could know that LCAT-positive cells survived and functioned for at least one month using the m-ccdPA transplanted mouse model.

The current study showed that implanted cells successfully supplied a therapeutic level of LCAT into the serum, and suggested the feasibility of the ccdPA-mediated gene therapy by use of ccdPA. However, there are remaining several issues to be dissolved before the clinical application, when we consider the cell implantation technique for various diseases other than LCAT deficiency. The first is the survival period of ccdPA after transplantation into the recipient. The precious model using insulin secreting adipocytes showed that the blood glucose-reducing activity was stably observed for two months (Ito et al., 2005). The stability of ccdPA needs to be evaluated for longer observation using the mice established in this study. The second is the unstable protein delivery by the transplanted ccdPA into serum at an initial phase to 7 days after subcutaneous transplantation, although the delivery became rather constant after the phase to a month. The characterization of transplanted ccdPA regarding the interaction between differentiation and secretion function is in progress using this model. Before obtaining the knowledge of multi-phase cell condition in recipient, the application of the cell therapy would be restricted to the enzyme deficiency without the over-dose toxicity in the enzyme-mediated metabolism in recipients. In order to dissolve the above remaining problem for wide clinical application, the established autologous cell transplantation model enables us to evaluate the effects of environmental condition of

transplanted cccdPA on the survival and/or functioin of cells in detail, which is critical for cell-based gene therapy in humans.

Refferences

Billings E Jr, May JW Jr (1989). Historical review and present status of free fat graft autotransplantation in plastic and reconstructive surgery. Plast Reconstr Surg 83, 368-381.

Bircoll M, Novack BH (1987). Autologous fat transplantation employing liposuction techniques. Ann Plast Surg. 18.327-329.

Cho SW, Kim I, Kim SH, Rhie JW, Choi CY, Kim BS (2006). Enhancement of adipose tissue formation by implantation of adipogenic-differentiated preadipocytes. Biochem Biophys Res Commun. 345, 588-594.

Coleman SR (2001). Structural fat grafts: the ideal filler? Clin Plast Surg 28, 111-119.

De Ugarte DA, Morizono K, Elbarbary A, Alfonso Z, Zuk PA, Zhu M, Dragoo JL, Ashjian P, Thomas B, Benhaim P, Chen I, Fraser J, Hedrick MH (2003). Comparison of multi-lineage cells from human adipose tissue and bone marrow. Cells Tissues Organs. 174.101-109

Dragoo JL, Samimi B, Zhu M, Hame SL, Thomas BJ, Lieberman JR, Hedrick MH, Benhaim P (2003). Tissue-engineered cartilage and bone using stem cells from human infrapatellar fat pads. J Bone Joint Surg Br. 85.740-747.

Fielding CJ, Fielding PE (1995). Molecular physiology of reverse cholesterol transport. J Lipid Res. 36, 211-228.

Gimble JM, Katz AJ, Bunnell BA (2007). Adipose-derived stem cells for regenerative medicine. Circ Res. 100.1249-1260.

Ito M, Bujo H, Takahashi K, Arai T, Tanaka I, and Saito Y (2005). Implantation of primary cultured adipocytes that secrete insulin modifies blood glucose levels in diabetic mice. Diabetologia 48, 1614-1620.

Jonas A (2000). Lecithin cholesterol acyltransferase. Biochim Biophys Acta. 1529, 245-256.

Kawaguchi N, Toriyama K, Nicodemou-Lena E, Inou K, Torii S, Kitagawa Y (1998). De novo adipogenesis in mice at the site of injection of basement membrane and basic fibroblast growth factor. Proc Natl Acad Sci U S A. 95.1062-1066.

Kimura Y, Ozeki M, Inamoto T, Tabata Y. (2003). Adipose tissue engineering based on human preadipocytes combined with gelatin microspheres containing basic fibroblast growth factor, Biomaterials 24.2513-2521.

Kitagawa Y, Kawaguchi N (1999). De novo adipogenesis for reconstructive surgery.

Cytotechnology. 31.29-35.

Kuramochi D, Unoki H, Bujo H, Kubota Y, Jiang M, Rikihisa N, Udagawa A, Yoshimoto S, Ichinose M, Saito Y (2008). Matrix metalloproteinase 2 improves the transplanted adipocyte survival in mice. Eur J Clin Invest. 38, 752-759.

Landazuri N, Krishna D, Gupta M, Le Doux JM (2007). Retrovirus-polymer complexes: study of the factors affecting the dose response of transduction. Biotechnol Prog. 23, 480-487.

Malafaya PB, Silva GA, Reis RL (2007). Natural-origin polymers as carriers and scaffolds for biomolecules and cell delivery in tissue engineering applications. Adv Drug Deliv Rev. 59, 207-233.

Mano JF, Silva GA, Azevedo HS, Malafaya PB, Sousa RA, Silva SS, Boesel LF, Oliveira JM, Santos TC, Marques AP, Neves NM, Reis RL (2007). Natural origin biodegradable systems in tissue engineering and regenerative medicine: present status and some moving trends. J R Soc Interface. 4, 999-1030.

Matsumoto F, Bujo H, Kuramochi D, Saito K, Shibasaki M, Takahashi K, Yoshimoto S, Ichinose M, Saito Y (2002). Effects of nutrition on the cell survival and gene expression of transplanted fat tissues in mice. Biochem Biophys Res Commun. 295. 630-635.

Mizuno H, Itoi Y, Kawahara S, Ogawa R, Akaishi S, Hyakusoku H (2008). In vivo adipose tissue regeneration by adipose-derived stromal cells isolated from GFP transgenic mice. Cells Tissues Organs. 187, 177-185.

Neuss S, Apel C, Buttler P, Denecke B, Dhanasingh A, Ding X, Grafahrend D, Groger A, Hemmrich K, Herr A, Jahnen-Dechent W, Mastitskaya S, Perez-Bouza A, Rosewick S, Salber J, Wöltje M, Zenke M (2008). Assessment of stem cell/biomaterial combinations for stem cell-based tissue engineering. Biomaterials. 29, 302-313.

Ning H, Liu G, Lin G, Yang R, Lue TF, Lin CS (2009). Fibroblast growth factor 2 promotes endothelial differentiation of adipose tissue-derived stem cells. J Sex Med. 6.967-979.

Patrick CW Jr (2000). Adipose tissue engineering: the future of breast and soft tissue reconstruction following tumor resection. Semin Surg Oncol. 19, 302-11.

Patrick CW Jr (2001). Tissue engineering strategies for adipose tissue repair. Anat Rec. 263.361-366.

Piasecki JH, Moreno K, Gutowski KA (2008). Beyond the cells: scaffold matrix character affects the in vivo performance of purified adipocyte fat grafts. Aesthet Surg J. 28.306-312.

Pinski KS, Roenigk FJU Jr (1992). Autologous fat transplantation. Long-term follow-up. J Dermatol Surg Oncol 18, 179-184.

Planat-Benard V, Silvestre JS, Cousin B, André M, Nibbelink M, Tamarat R, Clergue M, Manneville C, Saillan-Barreau C, Duriez M, Tedgui A, Levy B, Pénicaud L, Casteilla L (2004). Plasticity of human adipose lineage cells toward endothelial cells: physiological and therapeutic perspectives. Circulation. 109.656-663.

Rogachev, V.A., Likhacheva, A., Vratskikh, O., Mechetina, L.V., Sebeleva, T.E., Bogachev, S.S., Yakubov, L.A., and Shurdov, M.A. (2006). Qualitative and quantitative characteristics of the extracellular DNA delivered to the nucleus of a living cell. Cancer Cell Int. 6, 23.

Santamarina-Fojo, S., Hoeg, J.M., Assman, G., and Brewer, H.B. Jr. (2001). Lecithin cholesterol acyltransferase deficiency and fish eye disease. In: Scriver CR, Beaudet AL, Sly WS, Valle D, Childs B, Kinzler KW, and Volkman BF (eds). In The Metabolic and Molecular Bases of Inherited Disease, 8th edn. (McGraw-Hill Inc., New York) pp. 2817–2833.

Sugihara, H., Yonemitsu, N., Miyabara, S., and Yun, K. (1986). Primary cultures of unilocular fat cells: characteristics of growth in vitro and changes in differentiation properties. Differentiation 31, 42-49.

Sugihara, H., Yonemitsu, N., Miyabara, S., and Toda, S. (1987). Proliferation of unilocular fat cells in the primary culture. J. Lipid Res. 28, 1038-1045.

Stashower M, Smith K, Williams J, Skelton H (1999). Stromal progenitor cells present within liposuction and reduction abdominoplasty fat for autologous transfer to aged skin. Dermatol Surg. 25.945-949.

Tabata Y, Miyao M, Inamoto T, Ishii T, Hirano Y, Yamaoki Y, Ikada Y (2000). De novo formation of adipose tissue by controlled release of basic fibroblast growth factor. Tissue Eng. 6.279-289.

Torio-Padron N, Baerlecken N, Momeni A, Stark GB, Borges J (2007). Engineering of adipose tissue by injection of human preadipocytes in fibrin. Aesthetic Plast Surg. 31, 285-293.

Torio-Padron N, Borges J, Momeni A, Mueller MC, Tegtmeier FT, Stark GB (2007). Implantation of VEGF transfected preadipocytes improves vascularization of fibrin implants on the cylinder chorioallantoic membrane (CAM) model. Minim Invasive Ther Allied Technol. 16.155-162.

Tsuji W, Inamoto T, Yamashiro H, Ueno T, Kato H, Kimura Y, Tabata Y, Toi M (2009). Adipogenesis induced by human adipose tissue-derived stem cells. Tissue Eng Part A. 15.83-93.

Yamaguchi M, Matsumoto F, Bujo H, Shibasaki M, Takahashi K, Yoshimoto S, Ichinose M, Saito Y (2005). Revascularization determines volume retention and gene expression by fat grafts in mice. Exp Biol Med (Maywood). 230.742-748.

Yoshimura K, Asano Y, Aoi N, Kurita M, Oshima Y, Sato K, Inoue K, Suga H, Eto H, Kato H, Harii K (2009). Progenitor-Enriched Adipose Tissue Transplantation as Rescue for Breast Implant Complications.

Yoshimura K, Suga H, Eto H (2009). Adipose-derived stem/progenitor cells: roles in adipose tissue remodeling and potential use for soft tissue augmentation. Regen Med. 4.265-273.

Zuk PA, Zhu M, Mizuno H, Huang J, Futrell JW, Katz AJ, Benhaim P, Lorenz HP, Hedrick MH (2001). Multilineage cells from human adipose tissue: implications for cell-based therapies. Tissue Eng. 7.211-228.

Zuk PA, Zhu M, Ashjian P, De Ugarte DA, Huang JI, Mizuno H, Alfonso ZC, Fraser JK, Benhaim P, Hedrick MH (2002). Human adipose tissue is a source of multipotent stem cells. Mol Biol Cell. 13.4279-4295.

Figure legends

Figure 1. Enhanced gene transduction efficiency in m-ccdPA. Integrated copy numbers (A) and LCAT activity in the culture medium (B) after retrovirus vector mediated human *lcat* gene transduction were analyzed. Single round (b) and two rounds (a, c) of exposure to CGT_hLCATRV in the presence of 8 (a) or 500 μg/ml (b, c) of PS. Transduction with 8 μg/ml (a) and 500 μg/ml (b, c) of PS were performed overnight and one hour, respectively. Data are presented as the mean ± SD (n=3). *$p<0.05$.

Figure 2. Detection of human recombinant LCAT and survival of human *lcat* gene after transplantation of *lcat* gene-expressing m-ccdPA. Human *lcat* gene-transduced-mouse ccdPA (5 x 10^6 cells) were subcutaneously transplanted in nude mouse with fibrin glue as a scaffold. **A,** Existence of human LCAT protein in mice sera was detected by IP-western experiments. 15 μg human high density lipoprotein (HDL) was loaded for quantification of signals (H). Mouse serum with (PC) or without (NC) 15 μg HDL were subjected to IP-western. Serum (100 μl) from mouse transplanted with the gene transduced (T) and un-transduced (C) m-ccdPA were subjected to IP-western. **B,** Human *lcat* gene-transduced-mouse ccdPA (5 x 10^6 cells) were transplanted after three days culture with (open bars) or without (closed bars) adipogenic differentiation medium. The serum concentrations of the recombinant LCAT protein were quantified from densitometric analysis (left), and human *lcat* gene was quantified in excised implants

(right).

Figure 3. Detection of recombinant human LCAT in implants from mice. Sections of implants from the cells with transduced (A, B, and C) or un-transduced (D, E, F) by retrovirus vector at day28 were prepared and LCAT-immunostaining was performed. Implants were taken upon observation of PKH26 fluorescent. Immunohistochemical staining of human LCAT in fixed implants was done using rabbit anti-human LCAT monoclonal antibody as a primary antibody. Alexa Fluor 488 goat anti-rabbit IgG was used as a secondary antibody. The slides were counterstained with DAPI. Photographs of LCAT staining (A and D), DAPI staining (B and E), and merged images (C and F) were shown.

Figure 4. Effect of fibring glue on LCAT protein delivery. Human *lcat* gene transduced m-ccdPA were subcutaneously transplanted in CB57BL/6J mice using fibrin glue or Matrigel as scaffolds. Representative data of the experiment was shown (A), in which human LCAT delivery was monitored in single mouse. Concentrations of human LCAT protein in cell- transplanted mice sera with Matrigel (closed circle) or fibrin glue (closed triangle) were quantified by densitometric analysis after IP-western experiments (B).

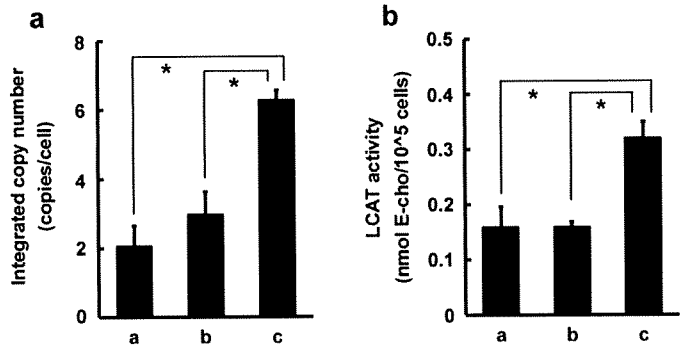

Figure 1.

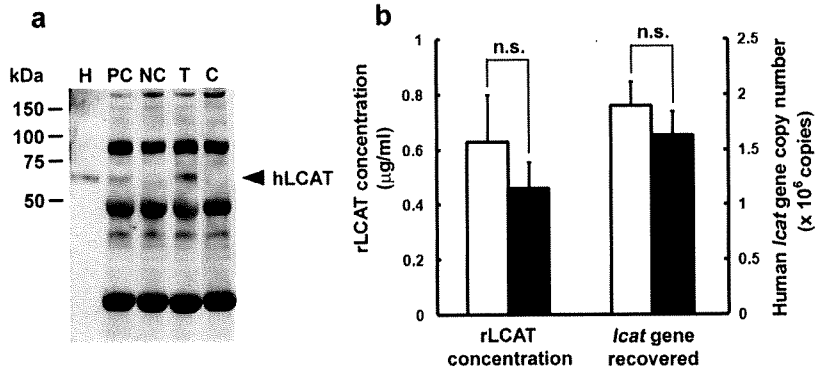

Figure 2.

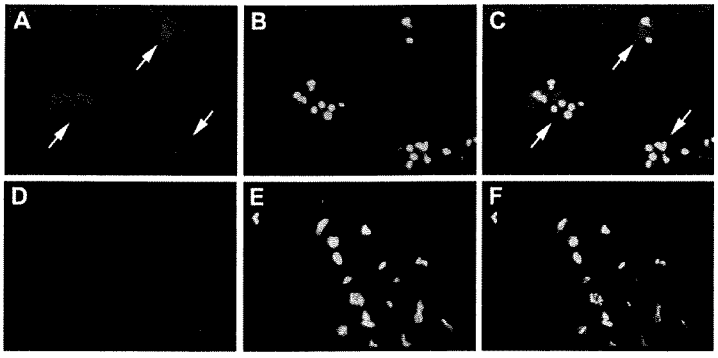

Figure 3.

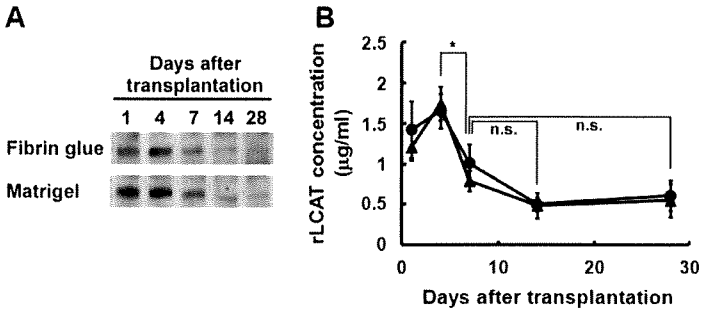

Figure 4.

Clinical Chemistry 55:10
1801–1808 (2009)

Development of an Immunoassay for the Quantification of Soluble LR11, a Circulating Marker of Atherosclerosis

Masanao Matsuo,[1] Hiroyuki Ebinuma,[1*] Isamu Fukamachi,[1] Meizi Jiang,[2] Hideaki Bujo,[2] and Yasushi Saito[3]

BACKGROUND: Vascular smooth muscle cells (SMCs) migrate from the arterial media to the intima in the progression of atherosclerosis, and dysfunction of SMCs leads to enhanced atherogenesis. A soluble form of the LDL receptor relative with 11 ligand-binding repeats (sLR11) is produced by the intimal SMCs, and the circulating concentrations of sLR11 likely reflect the pathophysiological condition of intimal SMCs. Furthermore, polymorphism of the LR11 gene has been found to be related to the onset of Alzheimer disease. This study describes the development of a sandwich immunoassay for quantifying sLR11 in human serum and cerebrospinal fluid.

METHODS: We used synthetic peptides or DNA immunization to produce monoclonal antibodies (MAbs) A2-2–3, M3, and R14 against different epitopes of LR11.

RESULTS: sLR11 was immunologically identified as a 250-kDa protein in human serum and cerebrospinal fluid by SDS-PAGE separation, and was purified from serum by use of a receptor-associated protein and MAb M3. An immunoassay for quantification of sLR11 with a working range of 0.25–4.0 μg/L was developed using the combination of MAbs M3 and R14. Treatment of serum with 5.25% n-nonanoyl-N-methyl-d-glucamine reduced the matrix effects of serum on the absorbance detection in the ELISA system. The linear dynamic range of the ELISA spanned the variation of circulating sLR11 concentrations in individuals with atherosclerosis.

CONCLUSIONS: A sandwich ELISA was established for quantifying sLR11 in serum and cerebrospinal fluid. This technique provides a novel means for assessing the pathophysiology of atherosclerosis, and possibly neurodegenerative diseases.

The LDL receptor relative with 11 ligand-binding repeats (LR11)[4] (also known as SorLA) *(1, 2)* is a member of the LDL receptor family and is highly expressed in atheromatous plaques, particularly in the intimal smooth muscle cells (SMCs) at the border between the arterial intima and the media *(3)*. Overproduction of LR11 protein promotes the enhanced migration of SMCs via the upregulation of urokinase-type plasminogen activator receptor *(4, 5)*. LR11 plays an essential role in the angiotensin II–induced mobility of SMCs, and angiotensin II type 1 receptor blockers have been found to reduce intimal thickness through the inhibition of the LR11/urokinase-type plasminogen activator receptor–mediated pathway of intimal SMCs in cuff-injured mice *(6)*. The extracellular domain of the membrane-spanning LR11 is released to yield an active soluble form of LR11 (sLR11) *(5, 7, 8)*. Recombinant sLR11 stabilizes urokinase-type plasminogen activator receptor and enhances the activation of the integrin/FAK/Rac1 pathway in SMCs and macrophages *(6, 8)*. The concentrations of sLR11 in arteries increased 2 weeks after endothelial injury in rats *(8)*, and the neutralization of sLR11 activity by specific antibodies reduced the intimal thickness after cuff injury in mice *(5)*. Statins, as well as angiotensin II type 1 receptor blockers, have been reported to inhibit the migration of intimal SMCs via the downregulation of LR11 expression and to attenuate LR11 expression in the intimal SMCs of aortic arteriosclerotic plaques in hyperlipidemic rabbits *(9)*.

Circulating sLR11 can be immunologically detected in serum by use of specific antibodies against LR11 *(6)*. Circulating concentrations of LR11 were positively correlated with intimal-media thickness in dyslipidemic individuals, and the correlation was independent of other classical risk factors for atherosclerosis *(6)*. In addition, neuronal LR11 expression is characteristically reduced in mild cognitive impairment and in the brains of individuals with Alzheimer disease (AD) *(10–13)*. Single nucleotide polymorphism anal-

[1] Tsukuba Research Institute, Sekisui Medical, Ibaraki, Japan; [2] Department of Genome Research and Clinical Application, Graduate School of Medicine, Chiba University, Chiba, Japan; [3] Department of Clinical Cell Biology, Graduate School of Medicine, Chiba University, Chiba, Japan.
* Address correspondence to this author at: Tsukuba Research Institute, Sekisui Medical, 3-3-1, Koyodai, Ryugasaki, Ibaraki 301-0852, Japan. Fax +81-297-62-8635; e-mail ebinuma002@sekisui.jp.

Received March 9, 2009; accepted July 9, 2009.
Previously published online at DOI: 10.1373/clinchem.2009.127027

[4] Nonstandard abbreviations: LR11, LDL receptor relative with 11 ligand-binding repeats; SMC, smooth muscle cells; sLR11, soluble form of LR11; AD, Alzheimer disease; MAb, monoclonal antibody; CSF, cerebrospinal fluid; RAP, receptor-associated protein; PBST, PBS with Tween.

ysis of the gene for LR11 [sortilin-related receptor, L(DLR class) A repeats-containing (*SORL1*)] has been used to predict AD onset *(14, 15)*.

In this study, we produced specific monoclonal antibodies (MAbs) that bind to intact sLR11 without prior purification. Using these antibodies, we developed a novel sandwich ELISA method to quantify circulating sLR11 concentrations in both serum and cerebrospinal fluid (CSF). This technique provides a means for quantifying sLR11 to be used potentially as a marker for atherosclerosis and a predictor of AD and other neurodegenerative diseases.

Materials and Methods

BIOLOGICAL SAMPLES

Human and animal sera were purchased from Tennessee Blood Services and Cosmo Bio, respectively. Commercial human CSF samples (n = 13) were obtained from Scipac. To evaluate the normal concentration range of circulating sLR11, human serum was obtained from 87 healthy normolipidemic individuals (41 males and 46 females), who gave informed consent for participation in this study, which was approved by the Human Investigation Review Committee of the Chiba University Graduate School of Medicine.

EXTRACTION OF sLR11 WITH A RECEPTOR-ASSOCIATED PROTEIN AFFINITY RESIN

Recombinant human receptor-associated protein (RAP) was prepared as a glutathione *S*-transferase fusion protein *(16)* and applied to a glutathione-Sepharose resin (GE Healthcare), which was used to extract sLR11 from serum. Briefly, samples were incubated overnight at 4 °C at a RAP affinity resin–to–sample volume ratio of 1:20, and the resin was packed into a separation column. The column was washed with 20 mmol/L Na,K-phosphate buffer (pH 7.2) containing 150 mmol/L NaCL, and sLR11 was eluted with 50 mmol/L sodium citrate buffer (pH 5.0) containing 150 mmol/L NaCl. The sLR11 from cultured human IMR32 cells was extracted with a RAP affinity resin as described previously *(5)*.

PREPARATION OF MAb BY SYNTHETIC PEPTIDE IMMUNIZATION

Anti-LR11 MAb for use in the immunoblot analyses of human and animal sera was prepared by immunizing mice with a synthetic peptide (SMNEENMRSVITFDKG) corresponding to amino acid residues 432–447 of LR11 *(2, 17)* coupled to keyhole-limpet hemocyanin. The peptide–keyhole-limpet hemocyanin complex was emulsified with complete Freund's adjuvant (Gibco) and subcutaneously injected into BALB/c mice, 4 times at 2-week intervals. The spleen cells extracted from the immunized mice were fused with mouse myeloma cells (Sp2/0) in the presence of 50% polyethylene glycol. A single clone was selected to yield MAb A2-2–3 (IgG1,k), which reacted with both human and rabbit sLR11 in immunoblot analyses.

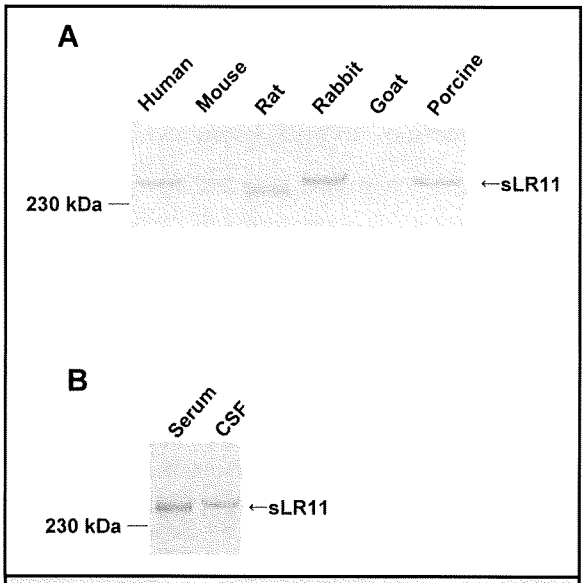

Fig. 1. Identification of sLR11 in serum and CSF.
(A), Samples (50 μL) extracted from human and animal sera by RAP affinity resin were separated by SDS-PAGE (2%–15% gradient) under reducing conditions. The sLR11 was detected by using an immunoblot assay with MAb A2-2–3. (B), Human CSF (10 μL) was separated by SDS-PAGE (2%–15% gradient) under reducing conditions, with RAP affinity-treated human serum as a control. The sLR11 protein was detected as above. A representative photo is shown. A 230-kDa marker is shown at the left in both panels.

IMMUNOBLOT ANALYSIS

Before immunoblot analysis, serum proteins were boiled in SDS-Tris buffer, with or without β-mercaptoethanol (reducing or nonreducing condition, respectively), and then separated by SDS-PAGE and transferred to a polyvinylidene difluoride membrane (Millipore). The membrane was blocked with 1% BSA in PBS containing 0.05% Tween 20 (PBST), incubated with MAb A2-2–3, reacted with horseradish peroxidase–conjugated rabbit antimouse IgG using a VECTASTAIN ABC kit (Vector Laboratories) according to the manufacturer's instructions, and subsequently stained with diaminobenzidine.

PREPARATION OF MAbs BY DNA IMMUNIZATION

Anti-LR11 MAbs for the sandwich ELISA were prepared via DNA immunization at Nosan Corporation *(18–20)*. Briefly, cDNA encoding amino acid resi-

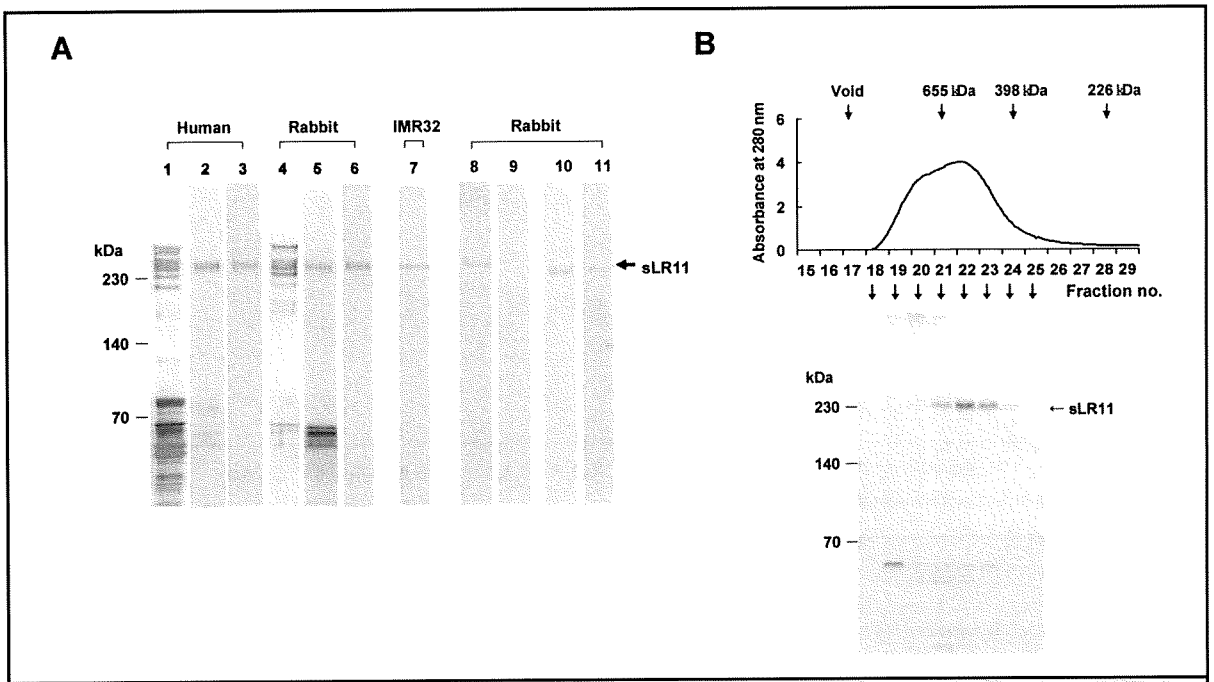

Fig. 2. Purification of sLR11 from human and rabbit serum.

(A), Samples extracted from a RAP affinity column with (lanes 2, 3, 5, 6, and 8–11) or without (lanes 1, 4, and 7) subsequent purification using an MAb-M3 affinity column were separated by SDS-PAGE (2%–15% gradient) under reducing (lanes 1–9) or nonreducing (lanes 10 and 11) conditions. Following electrophoresis, the samples were silver stained (lanes 1, 2, 4, and 5), or subjected to immunoblot analysis using MAb A2-2–3 (lanes 3, 6, and 7), R14 (lanes 8 and 10), or M3 (lanes 9 and 11). Lanes 1–3, human serum; lanes 4–6 and 8–11, rabbit serum; lane 7, human IMR32 cells. (B), Purified rabbit sLR11 protein was fractionated by gel filtration chromatography (HiLoad Superdex 200), and absorbance was monitored at 280 nm. The eluted proteins in each fraction were separated by SDS-PAGE under nonreducing conditions, and then silver stained. Markers at 230, 140, and 70 kDa are shown at the left.

dues 1000–1550 of LR11 *(2, 17)* was cloned into an expression plasmid (in-house vector, Nosan), and we immunized BALB/c mice or Wistar rats by intradermal application of DNA-coated gold particles, using a hand-held device for particle bombardment (Gene Gun, Bio-Rad). Antibody-producing cells were isolated and fused with Sp2/0 myeloma cells by use of polyethylene glycol, according to standard procedures. Five mouse and 5 rat MAbs were selected based on their reactivity with extracted rabbit sLR11, and preliminary sandwich ELISAs were performed using various combinations of these MAbs and A2-2–3. Mouse MAb M3 (IgG2a,k) and rat MAb R14 (IgG2b,k) were identified as the most sensitive for rabbit and human sLR11, respectively, and the combination of these antibodies gave the strongest reactivity against serum sLR11 in our ELISA system. Rat MAb R14 was then conjugated with sulfo-NHS-LC-biotin (Pierce), according to the manufacturer's instructions.

PURIFICATION OF sLR11 FROM HUMAN AND RABBIT SERA

The RAP affinity resin described above was used to extract sLR11 from 2.5 L of human serum or 1.0 L of rabbit serum. The eluted proteins were concentrated and applied to a HiLoad Superdex 200 gel filtration column (GE Healthcare) equilibrated with PBS. The fractions containing immunologically detected sLR11 were pooled, concentrated, and incubated overnight at room temperature with anti-LR11 MAb M3-Sepharose resin. After the resin was rinsed with PBS, immunologically bound sLR11 was eluted with 100 mmol/L sodium citrate buffer (pH 3.0). The sLR11 content was quantified by comparison with BSA standards on silver-stained gels.

SANDWICH ELISA

The wells of a polystyrene microtiter plate (Nunc) were coated with 100 μL of MAb M3 (10 mg/L in PBS) and incubated for 2 h. After extensive washing with PBST, the wells were blocked by incubation with 200 μL of

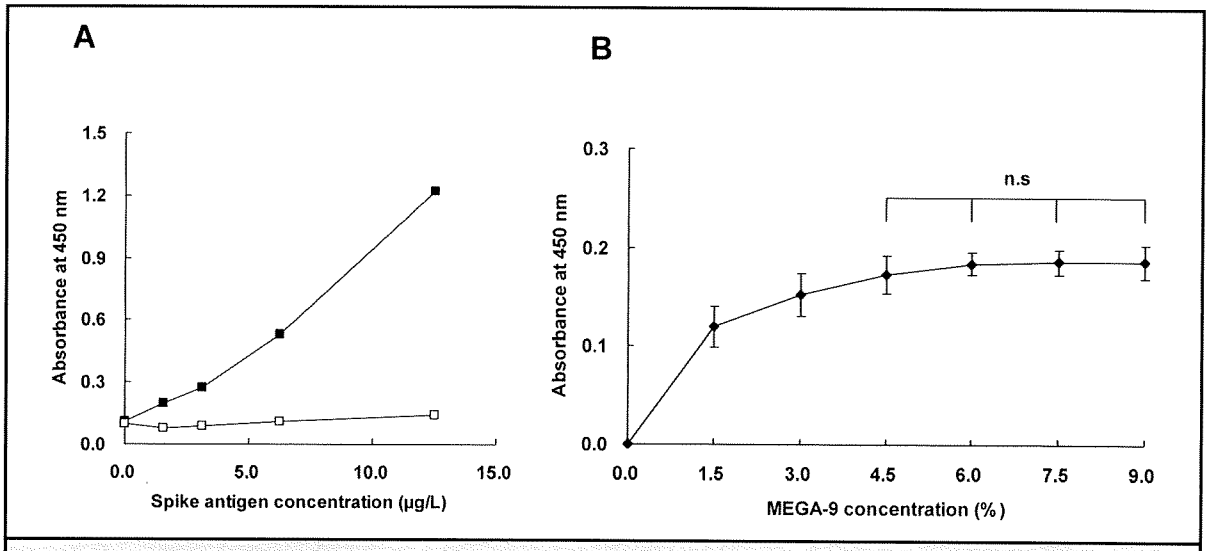

Fig. 3. The effect of MEGA-9 on ELISA measurements of sLR11 in the presence or absence of human serum.
(A), Extracted human sLR11 was measured by ELISA; sLR11 samples were diluted with PBS in the presence (□) or absence (■) of 10% human serum. (B), The sLR11 concentrations were quantified by ELISA (n = 8) in the sample buffer containing 10% human serum in the presence of various concentrations of MEGA-9. n.s., not significant.

1% BSA-PBST for 1 h. The samples (10 μL) were diluted with 100 μL of sample buffer, which consisted of 5.25% n-nonanoyl-N-methyl-d-glucamine (MEGA-9; Dojindo) and 25% heterophilic blocking reagent (Scantibodies Laboratory) in PBS. The calibration samples (0–4.0 μg/L rabbit sLR11) serially diluted in sample buffer together with the above diluted samples (100 μL) were placed into wells and then incubated for 6–16 h. After extensive washing with PBST, 100 μL of biotinylated MAb R14 was added to each well, and the plate was subsequently incubated for 4 h. After extensive washing with PBST, the LR11-MAb complex was reacted with horseradish peroxidase–conjugated streptavidin (Pierce) for 1 h. The trapped complexes were washed and incubated with 100 μL of substrate solution (tetramethyl-benzidine in citrate buffer, pH 3.65, containing hydrogen peroxide) for 30 min. The chromogenic reaction was stopped with 100 μL H_2SO_4, and the absorbance of each sample was determined at 450 nm. All steps were performed at room temperature. ELISA data (μg/L) were significantly and positively correlated with the immunoblotting data (U) previously observed following purification with RAP affinity chromatography ($r = 0.781$, $P < 0.001$, $y = 1.31x + 8.34$) *(6)*.

STATISTICAL ANALYSIS

Statistical analyses were performed with commercial software (Stat Flex, Ver. 5.0). The effect of sample dilution with various concentrations of MEGA-9 on the ELISA results was examined using a paired *t*-test, with $P < 0.05$ considered significant. The correlation between variables was evaluated using Pearson correlation analysis. Furthermore, sLR11 concentrations in individuals with atherosclerosis vs those in normal individuals were compared by use of box plot analysis.

Results

IDENTIFICATION OF sLR11 IN VARIOUS SERA AND HUMAN CSF

sLR11 was isolated as a 250-kDa protein from rabbit SMCs and human IMR32 cells by use of immunoblot techniques under reducing conditions and an antibody against a recombinant protein corresponding to a partial amino acid sequence of rabbit LR11 *(5)*. For comparison, sLR11 was extracted from both human and animal sera, using RAP–glutathione *S*-transferase resin. A single 250-kDa protein was detected in human serum by use of MAb A2-2–3 (Fig. 1A). The migration distance of the protein during electrophoresis was consistent with that of sLR11 from rabbit SMCs and human IMR32 cells *(5)*. A single protein band, similar in size to that obtained from human serum, was detected immunologically by MAb A2-2–3 in mouse, rat, rabbit, goat, and porcine sera. The relative intensities of the immunological signals suggested that sLR11 was most abundant in rabbit serum.

We also assessed the presence of sLR11 in human CSF (Fig. 1B), where it was identified by MAb A2-2–3 without the need for RAP extraction. Although sLR11

obtained from CSF was slightly larger than that in serum, the protein appeared as a single band at 250-kDa in both cases.

PURIFICATION OF sLR11 FROM HUMAN AND RABBIT SERA

Using DNA immunization, we established 2 MAbs, M3 and R14, against different epitopes of human sLR11; these MAbs were then used to purify intact sLR11 from serum and construct a sandwich ELISA assay. Intact sLR11 protein was first purified from human and rabbit sera using RAP affinity resin and was released from the resin with an eluting buffer, without decoupling from RAP–glutathione *S*-transferase (Fig. 2A, lanes 1 and 4). The eluted samples were treated with anti-LR11 MAb M3-Sepharose resin. Silver staining after electrophoresis indicated that the M3-reactive samples contained sLR11 as a single protein at 250 kDa as well as low molecular weight proteins, in both human and rabbit sera (lanes 2 and 5). The purified sLR11, but no other low molecular weight protein, was specifically bound to MAb A2-2–3 (lanes 3 and 6). The migration distance of sLR11 from human and rabbit sera was not different from that of sLR11 in the culture medium of IMR32 cells (lane 7). Therefore, 2-step affinity chromatography with RAP and MAb M3 can be used to specifically purify serum sLR11 as a soluble protein identical to that released from cultured cells. R14, as well as A2-2–3 and M3, showed reactivity against the purified sLR11, but did not bind any other low molecular weight protein (lanes 8–11). Notably, R14 reacted with sLR11 under both reducing and nonreducing conditions, whereas M3 reacted with sLR11 under nonreducing condition only.

Silver staining of the purified protein after gel filtration chromatography showed that the position to which purified sLR11 eluted corresponded to an estimated molecular weight >398 kDa (Fig. 2B). Notably, no other distinct protein proportional to the level of the stained sLR11 protein was detected in these fractions. The apparent molecular weight of sLR11 estimated from gel filtration was greater than that determined by use of gel electrophoresis (see Figs. 1 and 2A).

PREPARATION OF SAMPLES WITH MEGA-9 FOR SANDWICH ELISA

Sample conditions for the sandwich ELISA were determined using the above MAbs and purified samples. The absorbance level of immunologically detected sLR11 was proportional to the volume of extracted human sLR11 when diluted with PBS. However, the expected change in absorbance was not observed when samples were diluted with human serum instead of PBS (Fig. 3A). To measure sLR11 in human serum accurately, the matrix effects were mitigated by the addition of MEGA-9 detergent. The effects of MEGA-9 on absorbance recovery increased with increasing amounts

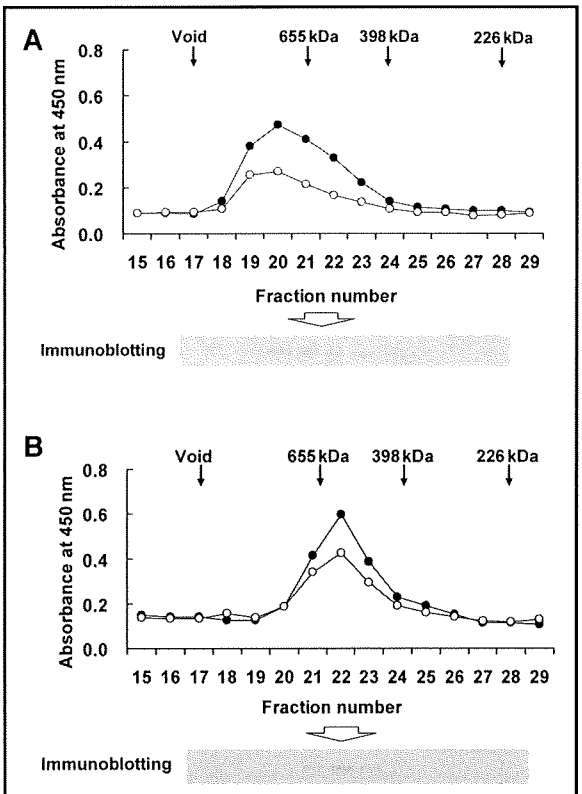

Fig. 4. Gel filtration elution profiles of sLR11 in human serum and CSF.

Human serum (A) and pooled CSF (B) samples (2 mL each) were fractionated by gel filtration chromatography (HiLoad Superdex 200), and the sLR11 concentration in each fraction was measured by ELISA in the presence (●) or absence (○) of MEGA-9. The amount of sLR11 in each fraction was also visualized by immunoblotting after extraction with the RAP affinity resin.

of MEGA-9, up to 4.5%. No significant differences were observed at higher concentrations (Fig. 3B). These results suggest that human serum contains unknown factors that interfere with sLR11 quantification, and that this interference could be diminished by the presence of MEGA-9. Therefore, samples were diluted with 5.25%, which was chosen as the middle concentration of 4.5% and 6.0%.

CHARACTERIZATION OF sLR11 IN SERUM AND CSF BY GEL FILTRATION

To assess whether ELISA can specifically detect naturally occurring sLR11, each fraction of human serum and CSF was analyzed for sLR11, following to separation by gel filtration chromatography; the results were then compared with the immunologically purified

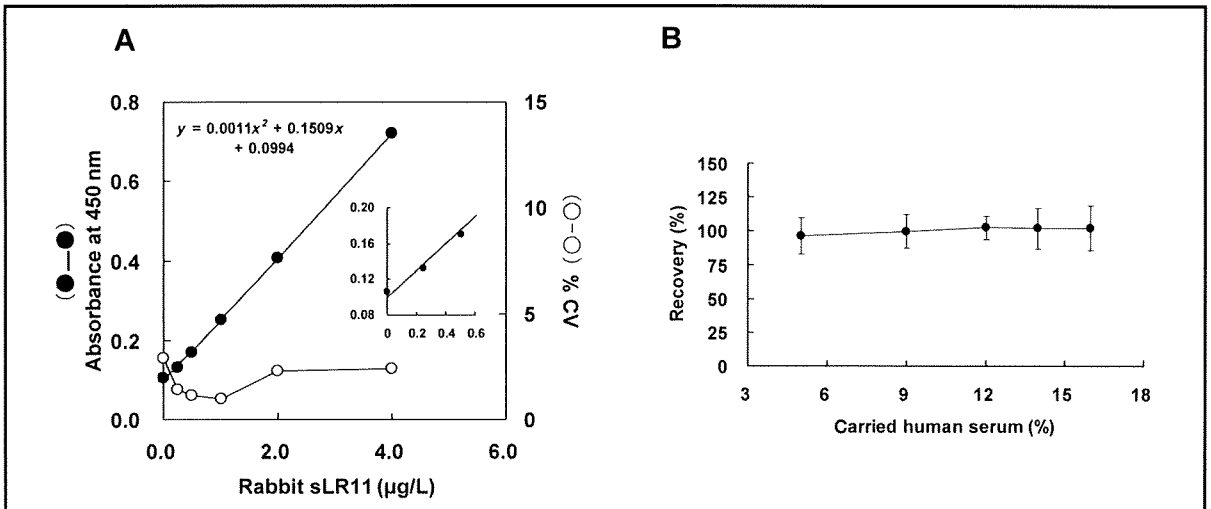

Fig. 5. Calibration curve and sample dilution test.

(A), Using the ELISA system developed in this study, we constructed a typical calibration curve (●) for sLR11 extracted from rabbit serum and the % CV of each point (○). Imprecision was assessed based on 5 replicates of the calibration curve. The insert graph is a close-up of the low-concentration area of the calibration curve. (B), Percentage recovery of purified sLR11 (2 μg/L) measured in the presence of various concentrations of human serum (5%–16%) in sample buffer. The concentration of each sample was measured using ELISA, and the percentage recoveries were calculated as a ratio of the actual-to-theoretical sLR11 concentrations.

sLR11 protein as a quantitative calibrator. The ELISA of serum and CSF samples that had been diluted with or without MEGA-9 showed abundant sLR11 in fractions with molecular weights >398 kDa (Fig. 4), similar to the results of the purified protein (see Fig. 2B). Immunoblot analyses showed that the concentration of sLR11 was proportional to the signal intensity of the gel-filtered 250-kDa proteins in both the serum and CSF samples. These results strongly suggest that this ELISA based on the immunologically purified 250-kDa sLR11 protein is also appropriate for quantifying the naturally occurring sLR11 in serum and CSF, although the gel filtration analyses suggested that the naturally occurring protein may be involved in a high molecular weight complex.

ELISA PERFORMANCE: ASSAY CHARACTERISTICS

A representative calibration curve is shown in Fig. 5A. The working range of this ELISA was 0.25–4.0 μg/L. A quadratic equation was applied to the calibration curve in the working range. The sensitivity, defined as the mean back-fit value for the lowest standard giving acceptable precision (CV = 10%), was 0.25 μg/L. With this ELISA method the lower limit of detection for sLR11 was 0.1 μg/L, which corresponds to the mean blank signal plus 3 SDs. The intraassay CVs (n = 10) were 3.0% and 3.7% at sLR11 concentrations of 7.6 μg/L in serum and 4.4 μg/L in CSF, respectively. The interassay CVs (n = 4) were 3.9% and 10.5% at sLR11 concentrations of 7.6 μg/L in serum and 4.1 μg/L in CSF, respectively. When we used samples containing 5%–16% human serum, percentage recovery ranged from 96.5% to 102.6% (Fig. 5B).

VARIATIONS OF sLR11 IN SERUM AND CSF

Measurements of sLR11 in 87 serum samples and 13 CSF samples obtained from normal individuals gave mean (SD) sLR11 concentrations of 8.7 (2.1) μg/L (range, 4.5–14.2 μg/L) and 8.5 (3.5) μg/L (range, 3.7–13.0 μg/L) in serum and CSF, respectively. We observed no significant difference in serum sLR11 concentrations between males [8.4 (1.9) μg/L, n = 41] and females [9.8 (5.8) μg/L, n = 46].

sLR11 CONCENTRATIONS IN INDIVIDUALS WITH ATHEROSCLEROSIS

To evaluate whether this ELISA method is useful for detecting variation in circulating sLR11 under pathophysiological conditions, we measured sLR11 concentrations in individuals with atherosclerosis. The sLR11 concentrations determined by immunoblotting after RAP affinity chromatography were positively correlated with the degrees of atherosclerosis in the carotid arteries of individuals with dyslipidemia *(6)*. The sLR11 concentrations in individuals with atherosclerosis were compared to those of healthy individuals (see

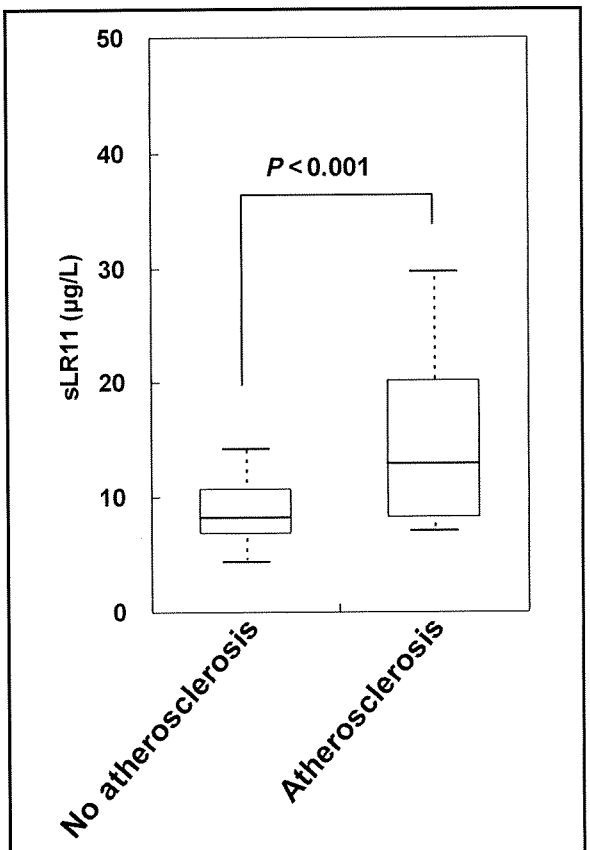

Fig. 6. Circulating sLR11 concentrations in individuals with atherosclerosis vs those in individuals without atherosclerosis.

Center horizontal lines indicate median values. Upper and lower edges of boxes, mean ± 1 SD; upper and lower bars, maximum and minimum.

previous section on variation of sLR11 in serum and CSF). The sLR11 concentrations [14.2 (6.0) μg/L] in individuals with atherosclerosis were significantly higher than those in healthy individuals (Fig. 6). The variation in circulating sLR11 concentrations in individuals with atherosclerosis was within the dynamic range of the ELISA.

Discussion

Three MAbs were established against different epitopes of human sLR11, and an ELISA method was developed for the quantitative measurement of sLR11 in serum and CSF. One of the MAbs (M3), in combination with RAP affinity extraction, enabled the purification of sLR11 from human and rabbit sera. The purified human and rabbit sLR11 was immunologically identical to sLR11 released from cultured cells, strongly suggesting that circulating sLR11 corresponds to the soluble form of membrane-bound LR11. This soluble form has been identified in the media of IMR32 and SMC cultures *(5, 6, 9)*. The combination of MAb M3 and MAb R14 yielded an ELISA that is highly specific for sLR11 in serum and CSF, without the need for prior RAP affinity extraction.

Strong matrix effects interfered with the accurate determination of sLR11 in serum by ELISA. However, these effects were diminished by pretreatment with MEGA-9 detergent (see Fig. 3). This pretreatment may dissociate complexes of sLR11 and serum components or may induce a conformational change in sLR11 such that it more efficiently interacts with the MAbs. Previous studies have shown that several serum components, including apolipoprotein E–containing lipoproteins, urokinase plasminogen activator–plasminogen activator inhibitor type 1 complex, and amyloid-β, can interact with membrane-bound LR11 *(1, 16, 21)*. The observation that MEGA-9 increased the absorbance of the isolated protein at 450 nm in gel filtration fractions obtained from both serum and CSF, and did so in proportion to the signal intensity of the sLR11 protein detected immunologically in the absence of MEGA-9 (see Fig. 4), suggests that epitope recognition by MAbs was strengthened by MEGA-9. The mechanism of MEGA-9–mediated absorbance enhancement requires further elucidation, specifically with regard to the interaction between naturally occurring sLR11 and various matrices in serum and with homomeric or heteromeric complexes under various column conditions (see Fig. 2B).

Using the established ELISA conditions, we investigated the mean sLR11 concentrations in serum and CSF. In 74% of healthy individuals, serum sLR11 concentrations were <10 μg/L. The sLR11 concentrations in the sera of individuals with atherosclerosis ranged from 6 to 30 μg/L. Therefore, the ELISA technique described here provides sufficient sensitivity for detecting circulating sLR11 concentrations in individuals with atherosclerosis and in normal populations.

Given that sLR11 is abundantly expressed in intimal SMCs *(3)* and that circulating sLR11 concentrations are positively correlated with the carotid intima-media thickness in dyslipidemic individuals *(6)*, variation in the circulating sLR11 concentration may be indicative of the condition of intimal SMCs. Metabolic disorders such as dyslipidemia and diabetes can cause pathological changes in intimal SMC function, possibly leading to accelerated progression of atherosclerosis *(22–24)*. The expression level of LR11 is drastically higher in intimal SMCs relative to that in medial SMCs *(3)*, and a large proportion of the LR11 in the cell membrane is released into the culture medium of

SMCs (5). Therefore, the concentration of circulating sLR11, rather than the LR11 expression level in intimal SMCs, may be more effective as a novel marker for pathogenic changes in SMCs.

Recent studies have highlighted the pathological function of sLR11 in neurodegenerative diseases. Immunological analyses indicate that sLR11 exists in CSF at concentrations similar to those in serum. Neuronal LR11 expression is significantly reduced in individuals with mild cognitive impairment and AD (10–13), and polymorphism of the gene for LR11 is highly associated with the onset of AD (14). Therefore, methods for determining sLR11 concentrations in CSF may be vital for future research into neuronal diseases, particularly AD.

In conclusion, we established a sensitive ELISA method for determining sLR11 concentrations in serum and CSF. This ELISA method constitutes a useful tool for monitoring the pathological condition of intimal SMCs and the progression of atherosclerosis (25). Use of this ELISA method to measure sLR11 as an indicator of intimal SMC function may enable novel strategies for treating atherosclerosis and help to determine risk factors for vascular disease. Furthermore, the ELISA described here has adequate sensitivity and dynamic range for determining sLR11 concentrations in CSF and may allow significant progress in AD-related research.

Author Contributions: *All authors confirmed they have contributed to the intellectual content of this paper and have met the following 3 requirements: (a) significant contributions to the conception and design, acquisition of data, or analysis and interpretation of data; (b) drafting or revising the article for intellectual content; and (c) final approval of the published article.*

Authors' Disclosures of Potential Conflicts of Interest: *No authors declared any potential conflicts of interest.*

Role of Sponsor: The funding organizations played no role in the design of study, choice of enrolled patients, review and interpretation of data, or preparation or approval of manuscript.

References

1. Yamazaki H, Bujo H, Kusunoki J, Seimiya K, Kanaki T, Morisaki N, et al. Elements of neural adhesion molecules and a yeast vacuolar protein sorting receptor are present in a novel mammalian low density lipoprotein receptor family member. J Biol Chem 1996;271:24761–8.
2. Jacobsen L, Madsen P, Moestrup SK, Lund AH, Tommerup N, Nykjaer A, et al. Molecular characterization of a novel human hybrid-type receptor that binds the α2-macroglobulin receptor associated protein (RAP). J Biol Chem 1996;271:31379–83.
3. Kanaki T, Bujo H, Hirayama S, Ishii I, Morisaki N, Schneider WJ, et al. Expression of LR11, a mosaic LDL receptor family member, is markedly increased in atherosclerotic lesions. Arterioscler Thromb Vasc Biol 1999;19:2687–95.
4. Zhu Y, Bujo H, Yamazaki H, Hirayama S, Kanaki T, Takahashi K, et al. Enhanced expression of the LDL receptor family member LR11 increases migration of smooth muscle cells in vitro. Circulation 2002;105:1830–6.
5. Zhu Y, Bujo H, Yamazaki H, Ohwaki K, Jiang M, Hirayama S, et al. LR11, an LDL receptor gene family member, is a novel regulator of smooth muscle cell migration. Circ Res 2004;94:752–8.
6. Jiang M, Bujo H, Ohwaki K, Unoki H, Yamazaki H, Kanaki T, et al. Ang II-stimulated migration of vascular SMC is dependent on LR11. J Clin Invest 2008;118:2733–46.
7. Böhm C, Seibel NM, Henkel B, Steiner H, Haass C, Hampe W. SorLA signaling by regulated intramembrane proteolysis. J Biol Chem 2006;281:14547–53.
8. Ohwaki K, Bujo H, Jiang M, Yamazaki H, Schneider WJ, Saito Y. A secreted soluble form of LR11, specifically expressed in intimal smooth muscle cells, accelerates formation of lipid-laden macrophages. Arterioscler Thromb Vasc Biol 2007;27:1050–6.
9. Jiang M, Bujo H, Zhu Y, Yamazaki H, Hirayama S, Kanaki T, et al. Pitavastatin attenuates the PDGF-induced LR11/uPA receptor-mediated migration of smooth muscle cells. Biochem Biophys Res Commun 2006;348:1367–77.
10. Andersen OM, Reiche J, Schmidt V, Gotthardt M, Spoelgen R, Behlke J, et al. Neuronal sorting protein-related receptor sorLA/LR11 regulates processing of the amyloid precursor protein. Proc Natl Acad Sci USA 2005;102:13461–6.
11. Scherzer CR, Offe K, Gearing M, Rees HD, Fang G, Heilman CJ, et al. Loss of apolipoprotein E receptor LR11 in Alzheimer disease. Arch Neurol 2004; 61:1200–5.
12. Dodson SE, Gearing M, Lippa CF, Montine TJ, Levey AI, Lah JJ. LR11/SorLA expression is reduced in sporadic Alzheimer disease but not in familial Alzheimer disease. J Neuropathol Exp Neurol 2006;65:866–72.
13. Sager KL, Wuu J, Leurgans SE, Rees HD, Gearing M, Mufson EJ, et al. Neuronal LR11/sorLA expression is reduced in mild cognitive impairment. Ann Neurol 2007;62:640–7.
14. Rogaeva E, Meng Y, Lee JH, Gu Y, Kawarai T, Zou F, et al. The neuronal sortilin-related receptor SORL1 is genetically associated with Alzheimer disease. Nat Genet 2007;39:168–77.
15. Cuenco KT, Lunetta KL, Baldwin CT, McKee AC, Guo J, Cupples LA, et al. Association of distinct variants in SORL1 with cerebrovascular and neurodegenerative changes related to Alzheimer disease. Arch Neurol 2008;65:1640–8.
16. Taira K, Bujo H, Hirayama S, Yamazaki H, Kanaki T, Takahashi K, et al. LR11, a mosaic LDL receptor family member, mediates the uptake of ApoE-rich lipoproteins in vitro. Arterioscler Thromb Vasc Biol 2001;21:1501–6.
17. Mörwald S, Yamazaki H, Bujo H, Kusunoki J, Kanaki T, Seimiya K, et al. A novel mosaic protein containing LDL receptor elements is highly conserved in humans and chickens. Arterioscler Thromb Vasc Biol 1997;17:996–1002.
18. Tang DC, DeVit M, Johnston SA. Genetic immunization is a simple method for eliciting an immune response. Nature 1992;356:152–4.
19. Krause S, Behrends J, Borowski A, Lohrmann J, Lang S, Myrtek D, et al. Blockade of interleukin-13-mediated cell activation by a novel inhibitory antibody to human IL-13 receptor alpha1. Mol Immunol 2006;43:1799–807.
20. Ikawa Y, Ng PS, Endo K, Kondo M, Chujo S, Ishida W, et al. Neutralizing monoclonal antibody to human connective tissue growth factor ameliorates transforming growth factor-b-induced mouse fibrosis. J Cell Physiol 2008;216:680–7.
21. Gliemann J, Hermey G, Nykjaer A, Petersen CM, Jacobsen C, Andreasen PA. The mosaic receptor sorLA/LR11 binds components of the plasminogen-activating system and platelet-derived growth factor-BB similarly to LRP1 (low-density lipoprotein receptor-related protein), but mediates slow internalization of bound ligand. Biochem J 2004;381:203–12.
22. Inaba T, Yamada N, Gotoda T, Shimano H, Shimada M, Momomura K, et al. Expression of M-CSF receptor encoded by c-fms on smooth muscle cells derived from arteriosclerotic lesion. J Biol Chem 1992;267:5693–9.
23. Tamura K, Kanzaki T, Tashiro J, Yokote K, Mori S, Ueda S, et al. Increased atherogenesis in Otsuka Long-Evans Tokushima fatty rats before the onset of diabetes mellitus: association with overexpression of PDGF beta-receptors in aortic smooth muscle cells. Atherosclerosis 2000;149:351–8.
24. Seki N, Bujo H, Jiang M, Tanaga K, Takahashi K, Yagui K, et al. LRP1B is a negative modulator of increased migration activity of intimal smooth muscle cells from rabbit aortic plaques. Biochem Biophys Res Commun 2005;331:964–70.
25. Bujo H, Saito Y. Modulation of smooth muscle cell migration by members of the low-density lipoprotein receptor family. Arterioscler Thromb Vasc Biol 2006;26:1246–52.

Atherosclerosis 204 (2009) 595–600

Contents lists available at ScienceDirect

Atherosclerosis

journal homepage: www.elsevier.com/locate/atherosclerosis

Plasma preβ1-HDL level is elevated in unstable angina pectoris

Jun Tashiro[a,c], Osamu Miyazaki[b,*], Yoshitake Nakamura[c], Akira Miyazaki[c], Isamu Fukamachi[b], Hideaki Bujo[d], Yasushi Saito[e]

[a] Department of Internal Medicine, Matsudo City Hospital, 4005, Kamihongo, Matsudo, Chiba 271-8511, Japan
[b] Tsukuba Research Institute, Sekisui Medical Co. Ltd. (Daiichi Pure Chemicals Co. Ltd.), 3-3-1, Koyodai, Ryugasaki, Ibaraki 301-0852, Japan
[c] Department of Cardiology, Chiba Cardiovascular Center, 575, Tsurumai, Ichihara, Chiba 290-0512, Japan
[d] Department of Genome Research and Clinical Application, Chiba University Graduate School of Medicine, 1-8-1, Inohana, Chuo-ku, Chiba 260-8670, Japan
[e] Department of Clinical Cell Biology, Chiba University Graduate School of Medicine, Chiba University, 1-8-1, Inohana, Chuo-ku, Chiba 260-8670, Japan

ARTICLE INFO

Article history:
Received 30 June 2008
Received in revised form 8 October 2008
Accepted 10 October 2008
Available online 1 November 2008

Keywords:
Preβ1-HDL
Acute coronary syndrome
HDL
Reverse cholesterol transport
LCAT

ABSTRACT

Preβ1-HDL, a minor HDL subfraction consisting of apolipoprotein A-I (apoA-I), phospholipids and unesterified cholesterol, plays an important role in reverse cholesterol transport. Plasma preβ1-HDL levels have been reported to be increased in patients with coronary artery disease (CAD) and dyslipidemia. To clarify the clinical significance of measuring plasma preβ1-HDL levels, we examined those levels in 112 patients with CAD, consisting of 76 patients with stable CAD (sCAD) and 36 patients with unstable angina pectoris (uAP), and in 30 patients without CAD as controls. The preβ1-HDL levels were determined by immunoassay using a specific monoclonal antibody (Mab55201) that we established earlier. The mean preβ1-HDL level in the CAD patients was significantly higher than the level in the controls (34.8 ± 12.9 mg/L vs. 26.6 ± 6.9 mg/L, $p < 0.001$). In addition, the mean preβ1-HDL level was markedly higher in the uAP subgroup than in the sCAD subgroup (43.1 ± 11.5 mg/L vs. 30.9 ± 11.7 mg/L, $p < 0.0001$). These tendencies remained even after excluding dyslipidemic subjects.

These results suggest that elevation of the plasma preβ1-HDL level is associated with the atherosclerotic phase of CAD and may be useful for identifying patients with uAP.

1. Introduction

Preβ1-HDL, an HDL subfraction consisting of one or two molecules of apolipoprotein A-I (apoA-I), small amounts of phospholipids and unesterified cholesterol, plays an important role in reverse cholesterol transport, although it comprises only 1–5% of total apoA-I in blood plasma [1–4]. The initial step of reverse cholesterol transport, called cholesterol efflux, is a reaction by which excessively accumulated cholesterol in peripheral tissues is removed by HDL. Preβ1-HDL is known as the initial plasma acceptor of cell-derived cholesterol [1–5].

Three pathways have been suggested as routes by which preβ1-HDL is generated [6–11]. The first is a pathway in which preβ1-HDL is formed when lipid-free apoA-I or lipid-poor apoA-I removes cell-derived, unesterified cholesterol, mediated by ATP-binding cassette transporter A1 (ABCA1) located on cell membranes [6–8]. The second is a pathway in which preβ1-HDL is directly secreted from the liver [9,10], and the third is a pathway in which preβ1-HDL is released from α-migrating HDL during its remodeling [11]. As the catabolic pathway of preβ1-HDL, a lecithin–cholesterol acyltransferase (LCAT)-dependent conversion pathway has been suggested. The unesterified cholesterol on the preβ1-HDL is esterified by LCAT, and the preβ1-HDL removes cellular cholesterols, increases in size and is converted to an α-migrating HDL [12–14].

Thus, preβ1-HDL is proposed to be a key component of reverse cholesterol transport. We previously reported development of a monoclonal antibody (Mab55201) specifically recognizing an epitope of apoA-I that is exposed only in preβ1-HDL, and we established an ELISA system for direct measurement of preβ1-HDL using Mab55201 [15]. The method provides a way to investigate the clinical significance of measuring plasma preβ1-HDL levels.

Plasma preβ1-HDL levels have been reported to be elevated in patients with coronary artery disease (CAD) and dyslipidemia [15–17]. However, the mechanism responsible for elevation of the preβ1-HDL level has not been clarified. In this study we examined whether the preβ1-HDL level is elevated in normolipidemic CAD patients and whether the levels differ between patients with unstable angina pectoris (uAP) and those with stable CAD (sCAD), including stable effort angina pectoris and old myocardial infarction. In addition, we studied the relationship between

* Corresponding author. Tel.: +81 297 62 6425; fax: +81 297 62 8635.
E-mail address: miyazaki084@sekisui.jp (O. Miyazaki).

0021-9150/$ – see front matter © 2008 Elsevier Ireland Ltd. All rights reserved.
doi:10.1016/j.atherosclerosis.2008.10.015

Table 1
Baseline characteristics of the study subjects.

	CAD (n = 112)	p^*	Normolipidemic CAD (n = 37)	p^*	Controls (n = 30)
Age (years)	65.8 ± 9.1	n.s.	65.5 ± 9.0	n.s.	66.3 ± 8.3
BMI (kg/m^2)	24.0 ± 2.7	n.s.	24.1 ± 3.4	n.s.	23.3 ± 2.9
SBP (mmHg)	127 ± 18.8	n.s.	123 ± 19.7	<0.05	134 ± 14.2
DBP (mmHg)	74.1 ± 11.7	n.s.	71.7 ± 12.5	<0.05	77.9 ± 9.7
HbA1c (%)	7.3 ± 1.4	<0.05	7.1 ± 1.4	n.s.	6.4 ± 1.2
T-Cho (mg/dL)	203 ± 41.4	n.s.	181 ± 22.9	n.s.	193 ± 20.3
TG (mg/dL)	142 ± 77.9	<0.001	92.2 ± 25.4	n.s.	85.3 ± 29.3
LDL-C (mg/dL)	131 ± 34.7	0.051	110 ± 21.7	n.s.	115 ± 16.1
HDL-C (mg/dL)	43.9 ± 9.4	<0.0001	49.8 ± 8.6	<0.05	55.2 ± 11.2
ApoA-I (mg/dL)	115 ± 18.5	<0.0001	123 ± 16.6	<0.01	137 ± 21.0
ApoB (mg/dL)	108 ± 27.3	<0.01	90.0 ± 16.1	n.s.	93.4 ± 12.3
Creatinine (mg/dL)	0.93 ± 0.32	<0.01	0.93 ± 0.34	<0.01	0.73 ± 0.18
BUN (mg/dL)	17.7 ± 7.3	n.s.	16.8 ± 4.0	n.s.	15.4 ± 4.0
AST (IU/L)	37 ± 19.5	n.s.	38.1 ± 16.3	n.s.	32.0 ± 11.0
ALT (IU/L)	27.4 ± 20.2	<0.05	29.1 ± 22.8	<0.05	19.0 ± 9.0
ChE (U/L)	325 ± 77.6	n.s.	308 ± 77.9	n.s.	316 ± 67.2
Medications, n (%)					
Aspirin	90(80.4%)	<0.0001	28(75.7%)	<0.0001	2(6.7%)
Nitrates	87(77.7%)	<0.0001	24(64.9%)	<0.0001	1(3.3%)
Calcium channel blockers	51(45.5%)	n.s.	17(45.9%)	n.s.	13(43.3)
Beta blockers	37(33.0%)	n.s.	10(27.0%)	n.s.	5(16.7%)
ACE inhibitors	26(23.2%)	n.s.	8(21.6%)	n.s.	3(10.0%)
Diuretics	10(8.9%)	n.s.	3(8.1%)	n.s.	1(3.3%)
Digoxin	6(5.4%)	n.s.	0(0.0%)	n.s.	1(3.3%)
ARBs	2(1.8%)	n.s.	1(2.7%)	n.s.	1(3.3%)
Antiplatelet	27(24.1%)	<0.01	9(24.3%)	<0.01	0(0.0%)
Antidiabetics	45(40.2%)	n.s.	13(35.1%)	n.s.	9(30.0%)
Lipid-lowering agents	3(2.7%)	n.s.	1(2.7%)	n.s.	0(0.0%)

Data are shown as mean ± S.D. or number. ARBs: angiotensin II receptor blockers.
* Significance vs. controls.

the preβ1-HDL level and lipid metabolism by examining for correlations between the preβ1-HDL level and the concentrations or activities of various lipid metabolic markers.

2. Methods

2.1. Study subjects

One hundred and twelve coronary artery disease patients were recruited from inpatients and outpatients of Chiba Cardiovascular Center (Chiba, Japan). The diagnosis of CAD was based on a history of myocardial infarction, clinical symptoms including prolonged chest pain, and the presence of angiographically demonstrated stenosis (≥75% obstructive lesions). The CAD group was divided into 36 patients with uAP and 76 patients with sCAD based on the clinical symptoms. uAP was diagnosed in accordance with the American Heart Association (AHA) classification (1975): the presence of chest pain which began during the previous 3 weeks and most recently occurred within the previous 1 week; and the absence of both ST segment elevation on the electrocardiogram and serum biochemical markers of cardiac necrosis. All patients with uAP belonged to class I or II in severity and class B or C in the clinical circumstances according to Braunwald's classification (1989). The sCAD subgroup was composed of 32 patients with stable effort angina pectoris and 44 patients with old myocardial infarction. We also enrolled 30 age- and BMI-matched subjects as the control group. The control subjects were recruited from outpatients of Chiba Cardiovascular Center and included type 2 diabetics and/or hypertension patients without dyslipidemia and no history of CAD. The control subjects were all confirmed to have no cardiac disorders on the exercise-loaded electrocardiogram. Normolipidemic subjects in the CAD group and the control group were determined on the basis of the concentrations of four serum lipid markers, i.e., total cholesterol (T-Cho) <220 mg/dL, LDL-cholesterol (LDL-C) <140 mg/dL, triglyceride (TG) <150 mg/dL, and HDL-cholesterol (HDL-C) ≥40 mg/dL. Patients with renal and/or liver dysfunction were excluded from this study.

We obtained informed consent from all participants at entry. This study was conducted in accordance with the Declaration of Helsinki of the World Medical Association.

2.2. Blood collection

Venous blood samples for plasma and serum were drawn from the subjects after fasting for one night. The blood samples for plasma were drawn into plastic tubes containing EDTA-2Na, immediately chilled in ice water and centrifuged at 2 °C. The plasma was diluted with 20 volumes of 50% sucrose solution for stabilization and then stored at −80 °C until preβ1-HDL was assayed. The blood samples for serum were separated and stored at −80 °C until assay for serum lipids, apolipoproteins, LCAT activity and other markers of liver or renal function.

2.3. Measurement of preβ1-HDL and biochemical parameters

Preβ1-HDL levels were measured by a sandwich enzyme immunoassay using Mab55201 [15,18]. The preβ1-HDL level was expressed as both an absolute value and a relative value. The absolute value indicates the preβ1-HDL concentration (mg/L) in the plasma, and the relative value indicates the percentage of preβ1-HDL in the total apolipoprotein A-I in the plasma.

The T-Cho, TG, LDL-C, HDL-C, creatinine, blood urea nitrogen (BUN), aspartate transaminase (AST), alanine transaminase (ALT) and cholinesterase (ChE) concentrations were determined enzymatically using an automated analyzer. Apolipoprotein concentrations were determined by immunoturbitometry with commercial reagents from Daiichi Pure Chemicals (Tokyo, Japan), using an automated analyzer. Hemoglobin A1c (HbA1c) was determined by an automated liquid-chromatographic system. LCAT

Table 2
Comparisons of preβ1-HDL levels between CAD and control groups and between uAP and sCAD subgroups.

	n	Preβ1-HDL (mg/L)	p	Preβ1-HDL/apoA-I (%)	p
CAD	112	34.8 ± 12.9	<0.001*	3.05 ± 1.04	<0.0001*
Normolipidemic CAD	37	36.2 ± 12.8	<0.001*	2.94 ± 0.95	<0.0001*
CAD (HDL-C ≥ 40 mg/dL)	74	36.9 ± 13.1	<0.0001*	2.98 ± 0.97	<0.0001*
CAD (high LCAT**)	28	36.5 ± 12.3	<0.001*	3.15 ± 0.93	<0.0001*
Controls	30	26.6 ± 6.9	–	1.97 ± 0.51	–
uAP	36	43.1 ± 11.5	<0.0001	3.66 ± 0.95	<0.0001
sCAD	76	30.9 ± 11.7		2.76 ± 0.95	
Normolipidemic					
uAP	16	43.1 ± 9.1	<0.01	3.42 ± 0.76	<0.01
sCAD	21	30.9 ± 12.8		2.58 ± 0.94	
HDL-C ≥ 40 mg/dL					
uAP	26	44.9 ± 11.6	<0.0001	3.54 ± 0.87	<0.001
sCAD	48	32.6 ± 11.9		2.68 ± 0.89	
HDL-C < 40 mg/dL					
uAP	10	38.3 ± 10.3	<0.05	4.00 ± 1.10	<0.01
sCAD	28	28.1 ± 11.0		2.90 ± 1.05	

Data are shown as mean ± S.D.
* Significance vs. controls.
** LCAT activity ≥80 nmol/mL/h/37 °C.

activities were determined only in 58 randomly selected CAD (9 uAP and 49 sCAD) patients, by the method of Nagasaki and Akanuma using an endogenous substrate [19].

2.4. Statistics

Statistical analyses were performed using Stat Flex for Windows ver. 5.0 (Artech Inc., Osaka, Japan). The difference between two groups was assessed using Student's paired *t*-test. Categorical variables were compared using the χ^2-test. The relationship between two parameters was examined using Pearson's Correlation Coefficient. Receiver-operating characteristic (ROC) curves were plotted, and the area under the curve (AUC) was analyzed to compare the predictive powers of preβ1-HDL, HDL-C and LDL-C for uAP using the sCAD and the control group as reference groups. The AUC indicates the diagnostic accuracy of tests [20]. For all analyses, $p < 0.05$ was considered statistically significant.

Table 3
Comparisons of baseline characteristics between sCAD and uAP subgroups.

	uAP (n = 36)	sCAD (n = 76)	p
Age (years)	67.0 ± 8.8	65.3 ± 9.2	n.s.
BMI (kg/m^2)	24.6 ± 3.4	23.8 ± 2.4	n.s.
SBP (mmHg)	129 ± 22.3	126 ± 16.9	n.s.
DBP (mmHg)	76.8 ± 13.5	72.9 ± 10.7	n.s.
HbA1c (%)	7.5 ± 1.3	7.3 ± 1.4	n.s.
T-Cho (mg/dL)	191 ± 41.8	209 ± 40.2	<0.05
TG (mg/dL)	129 ± 67.4	147 ± 82.1	n.s.
LDL-C (mg/dL)	118 ± 35.6	132 ± 33.5	<0.05
HDL-C (mg/dL)	44.4 ± 9.8	43.6 ± 9.2	n.s.
ApoA-I (mg/dL)	119 ± 20.3	112 ± 17.3	n.s.
ApoB (mg/dL)	100 ± 26.3	112 ± 27.0	<0.05
Creatinine (mg/dL)	0.96 ± 0.29	0.91 ± 0.34	n.s.
BUN (mg/dL)	17.7 ± 4.8	17.8 ± 8.2	n.s.
AST (IU/L)	39.8 ± 21.2	35.7 ± 18.7	n.s.
ALT (IU/L)	28.6 ± 20.6	26.9 ± 20.1	n.s.
ChE (U/L)	30.5 ± 89.8	335 ± 69.6	n.s.
LCAT activity (nmol/mL/h/37 °C)*	72.9 ± 21.0	72.9 ± 12.4	n.s.
Medications, n (%)			
Aspirin	28 (77.8%)	62 (81.6%)	n.s.
Nitrates	27 (75.0%)	60 (78.9%)	n.s.
Calcium channel blockers	16 (44.4%)	35 (46.1%)	n.s.
Beta blockers	12 (33.3%)	25 (32.9%)	n.s.
ACE inhibitors	10 (27.8%)	16 (21.1%)	n.s.
Diuretics	4 (11.1%)	6 (7.9%)	n.s.
Digoxin	1 (2.8%)	5 (6.6%)	n.s.
ARBs	0 (0.0%)	2 (2.6%)	n.s.
Antiplatelet	11 (30.6%)	16 (21.1%)	n.s.
Antidiabetics	9 (25.0%)	36 (47.4%)	<0.05
Lipid-lowering agents	1 (2.8%)	2 (2.6%)	n.s.

Data are shown as mean ± S.D. or number (%). ARBs: angiotensin II receptor blockers.
* Determined in 9 uAP and 49 sCAD patients.

3. Results

3.1. Comparison between CAD patients and controls

Table 1 shows the baseline characteristics of the study subjects. Age, BMI and blood pressure were comparable between the CAD and control groups. The concentrations of HbA1c, TG and apoB were significantly higher, and the concentrations of HDL-C and apoA-I were significantly lower, in the CAD group than in the control group. In the normolipidemic subjects, the only differences were that the concentrations of HDL-C and apoA-I were slightly higher in the control group. Medications were comparable between the CAD and control groups except for aspirin, nitrates and antiplatelet drugs. The absolute and relative values for the preβ1-HDL level were markedly higher in the CAD group than in the control group. These differences were also seen even in the normolipidemic subjects only (Table 2). We then compared the preβ1-HDL levels between the CAD subgroups with high HDL-C (≥40 mg/dL) or high LCAT activity (≥80 nmol/mL/h/37 °C) and the control group. The preβ1-HDL levels were markedly higher in both the CAD subgroups than in the control group (Table 2).

3.2. Comparison between uAP and sCAD subgroups

We divided the CAD group into a uAP subgroup and an sCAD subgroup and compared the preβ1-HDL levels between them. The absolute and relative values for the preβ1-HDL level were markedly higher in the uAP subgroup than in the sCAD subgroup. Moreover, even in the comparisons using only the normolipidemic subjects, only the high HDL-C (≥40 mg/dL) subjects and only the low HDL-C (<40 mg/dL) subjects, the differences remained significant between the two subgroups (Table 2). On the other hand, the concentrations of lipid markers, age, BMI, blood pressure, renal and hepatic function markers and medications did not differ between the uAP and

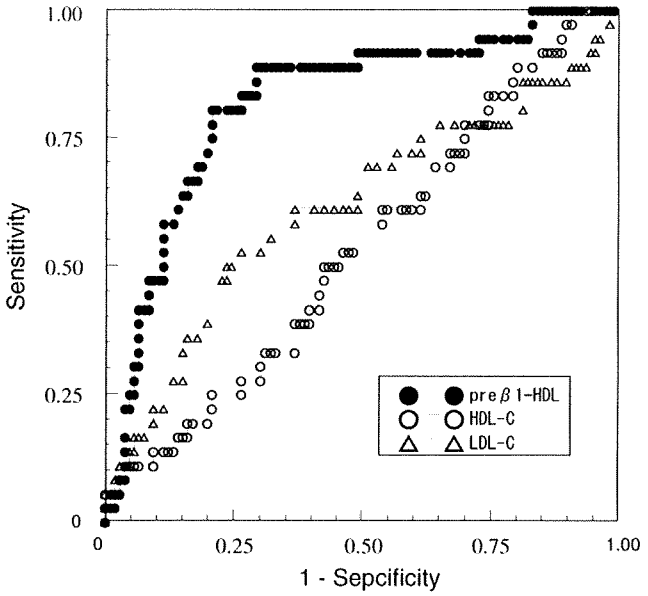

Fig. 1. ROC curves of preβ1-HDL, HDL-C, LDL-C for diagnosis of uAP. The true-positive rate (sensitivity as *y* axis) was plotted vs. the false-positive rate (1-specificity as *x* axis) by changing the cutoff values for the test. The areas under the curves were 0.821 (95% CI, 0.780–0.863) for preβ1-HDL, 0.536 (95% CI, 0.482–0.591) for HDL-C and 0.616 (95% CI, 0.557–0.675).

Table 4
Correlations between preβ1-HDL and clinical factors.

	CAD group (n = 112)		Control group (n = 30)	
	r	p	r	p
Age	0.163	n.s.	−0.122	n.s.
BMI	0.134	n.s.	−0.026	n.s.
SBP	−0.037	n.s.	0.117	n.s.
DBP	0.003	n.s.	0.115	n.s.
HbA1c	0.127	n.s.	−0.039	n.s.
T-Cho	0.146	n.s.	−0.013	n.s.
TG	0.200	<0.05	−0.157	n.s.
LDL-C	0.025	n.s.	−0.054	n.s.
HDL-C	0.247	<0.01	0.194	n.s.
ApoA-I	0.400	<0.0001	0.189	n.s.
ApoB	0.070	n.s.	−0.157	n.s.
Creatinine	0.172	n.s.	−0.012	n.s.
BUN	0.183	n.s.	0.181	n.s.
AST	0.182	n.s.	0.035	n.s.
ALT	0.207	<0.05	−0.195	n.s.
ChE	0.068	n.s.	−0.033	n.s.
LCAT activity*	0.204	n.s.	–	–

* Determined in 58 CAD patients.

sCAD subgroups, except that the concentrations of T-Cho, LDL-C and apoB were slightly lower and that the patients taking antidiabetics were slightly fewer in number in the uAP subgroup (Table 3).

3.3. *Preβ1-HDL as a diagnostic marker of uAP*

ROC analyses were performed to evaluate preβ1-HDL as a diagnostic marker of uAP. The AUC of preβ1-HDL was significantly greater than that of either HDL-C or LDL-C (vs. HDL-C, $p < 0.0001$; vs. LDL-C, $p < 0.01$) (Fig. 1).

3.4. *Correlations between preβ1-HDL level and clinical factors*

We examined for correlations between the absolute preβ1-HDL concentration and various clinical factors in the CAD patients and in the control subjects. In the CAD patients, the preβ1-HDL concentration showed a strong, significant positive correlation with apoA-I and a significant positive correlation with HDL-C. On the other hand, no correlation was found with the LDL-C, T-Cho or LCAT activity. TG showed a slightly positive correlation with preβ1-HDL. The only other marker correlating significantly with preβ1-HDL was ALT, which correlated slightly. In the control subjects, none of the factors showed a significant correlation with preβ1-HDL (Table 4).

We then examined for correlations between the preβ1-HDL and the HDL-C, apoA-I or LCAT activity in the uAP and sCAD subgroups separately. HDL-C showed a significant positive correlation with preβ1-HDL in the sCAD subgroup, but not in the uAP subgroup (Fig. 2A). ApoA-I showed a significant positive correlation with preβ1-HDL in both the uAP and sCAD subgroups (Fig. 2B), whereas LCAT activity did not (Fig. 2C).

4. Discussion

The present study clearly showed that the plasma preβ1-HDL level was high in the CAD group even when excluding dyslipidemic patients (Table 2). Earlier studies reported the plasma preβ1-HDL concentration to be elevated in patients with CAD, dyslipidemia and obesity, and also in hemodialysis patients [15–17,21,22]. The present study excluded patients with renal disorders, including hemodialysis patients, and BMI-matched control subjects were

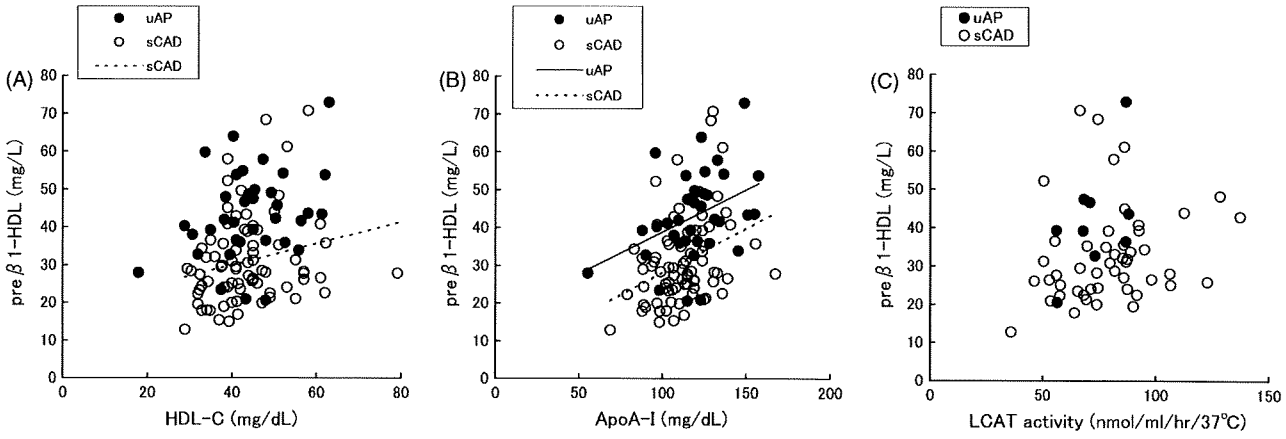

Fig. 2. Correlations (Pearson's Coefficients) between preβ1-HDL levels and HDL-C levels (A), apoA-I levels (B) and LCAT activities (C) in uAP and sCAD subgroups. A: uAP (n = 36), r = 0.313, p = 0.063; sCAD (n = 76), r = 0.227, $p < 0.05$. B: uAP (n = 36), r = 0.394, $p < 0.05$; sCAD (n = 76), r = 0.350, $p < 0.01$. C: uAP (n = 9), r = 0.538, p = 0.135; sCAD (n = 49), r = 0.215, p = 0.139.